JNEST EISSN: 2961-8738 ● PISSN: 2961-8916 ● DOI: 10.56741/jnest.v5i03.2480
Article Received 04 July 2026, Revised 28 August 2026

Influence of U-Shape Row Pile Configuration to Mitigate Steep Slope Failure: A Numerical Study

Muhammad Chofi Irnawan, Muhammad Shofwan Donny Cahyono*

***Abstract*—Landslide is a major problem in the field of geotechnical engineering, particularly in steep areas such as mountainous regions. In areas with steep topography, soil masses or rocks are unable to withstand the force of gravity and external forces acting on the slope, resulting in the movement of rock and soil. These materials move down the slope in the form of fragments, flows, and cascades over a wide area. Therefore, reinforcement is required to prevent collapse. One commonly used reinforcement method is pile. The pile installation patterns frequently employed are parallel arrangements in single and double rows. However, there has been no installation using a U-shaped configuration. Thus, this study aims to numerically analyze the stability of a slope reinforced with piles in a U-shaped configuration and compare it with the existing slope conditions without reinforcement. The method used is finite element analysis with the strength reduction method (SRM). The software used in the numerical analysis is Plaxis 2D. The results of SRM numerical analysis show that reinforcement with a double contiguous U-shaped pile system is capable of improving slope stability. This is indicated by an increase in the safety factor (FoS) value of up to 57% compared to the unreinforced slope.**

***Index Terms*— Finite Element Analysis, Plaxis, Reinforcement, Safety Factor, Slope Stability, Strength Reduction Method**

I. Introduction

Landslides are one of the major issues in geotechnical engineering, particularly in steep areas such as mountainous regions. In areas with steep topography, masses of soil or rock are unable to withstand the force of gravity and external forces acting on the slope, resulting in the movement of rock and soil. These materials move down the slope in the form of blocks, flows, and falls over a wide area [1]. The impacts caused by slope failures include damage to facilities such as roads, railways, buildings, and infrastructure [2].

The primary causes triggering slope instability include geomorphology, variations in geological and structural elements (weak rock, debris flows, weak soils, shear bands, and faults), as well as massive slope cutting resulting from human activities [3]. Additionally, other factors contributing to slope failure include slope mass geometry, stress-strain history, external loads, regional climate, seismic activity, pore water pressure conditions, and geostructure. These factors are used to determine the potential extent of the slip plane and to identify the behaviour of the sliding mass on the slope. Common failure patterns on slopes include planar, circular, and spiral log patterns. Slope failure will not occur if the stress caused by external loads is less than the strength of the soil [4].

The efforts to address slope failures involve adding reinforcement. The purpose of adding reinforcement is to ensure the reliability, stability, and safety of slopes in projects such as mining, highways, and hydroelectric power plants. In field practice, the slope reinforcement methods commonly used are geocells and vegetation, geogrids, and gabions [5]–[6]. However, the use of these materials presents challenges, such as a decrease in the effectiveness of geogrid reinforcement as vertical stress increases due to a steeper slope gradient [7]. Additionally, the long-term use of gabions may lead to shear failure caused by scouring. Scouring causes erosion and reduces passive resistance at the toe, thereby decreasing the safety factor (FoS) of the slope [8]. Therefore, researchers recommend the stronger and more reliable protection methods, such as ground anchors, soil nailing, and piles. The use of these materials can significantly improve slope stability by increasing the FoS value under both static and dynamic load conditions [9]–[11]. There are several patterns that can be used to reinforce slopes, namely single-row and double-row. However, the more complex the installation pattern and the greater the variation in pile shapes, the greater the complexity in the analytical calculation process. Consequently, specialized methods are required to address the problems.

The Limit Equilibrium Method (LEM) is a conventional analytical method used in slope stability analysis to determine whether a soil or rock slope is stable against failure. The main principle involves the equilibrium of horizontal forces or moments to determine the safety factor (FoS) [12]. Popular LEM-based analysis method has been proposed by Fellenius, Bishop, Morgenstern and Price, Spencer, Janbu, and Sarma. Although LEM analysis is still considered a valid method for slope stability analysis in determining the safety factor, it has limitations in estimating the shape of the failure surface and the forces acting at the intersections of the sections [13].

Consequently, experts have sought to adopt more effective methods for predicting slope failure, namely two Finite Element Methods: Enhanced Limit Strength Method (ELSM) and Strength Reduction Method (SRM). The SRM has been used for slope stability analysis since the early 1970s. This method allows for the use of various constitutive models, such as elastic, plastic, and elastoplastic, enabling the detection of failure movements up to the stage of total collapse. SRM also provides more detailed and accurate representation of soil behaviours, such as the transition of soil properties from homogeneous linear isotropic to nonlinear heterogeneous anisotropic, and is capable of analysing models that cannot be addressed using conventional calculation methods.

Muhammad Chofi Irnawan and **Muhammad Shofwan Donny Cahyono** (Corresponding Author) are with the Department of Civil Engineering, Universitas Widya Kartika, Surabaya, Indonesia. Corresponding author: *shofwandonny@widyakartika.ac.id

© 2026 IISTR

Furthermore, the key advantage of SRM is that the slip surface is automatically identified from the shear strain, which increases as the shear strength decreases. Over the past 10 years, the Finite Element Method (FEM) has become the most popular method. In its application, FEM analysis utilizes software such as Plaxis, Abaqus, and Ansys [14]–[16].

Researchers have conducted studies on the FEM for the stability of slopes reinforced with piles [17]–[18]. One such study, by Wei and Chen [19], evaluated the effect of installing a single row of piles on an earthen slope with spacing variations ranging from two times the diameter (2D) to eight times the diameter (8D). The results of the simulation showed that single-row pile installation was able to increase the FoS value. However, the greater distance between piles caused a decrease in the slope's FoS value. Shooshpasha and Amirdehi [20] examined the effect of single-row pile installation with variations in pile length and spacing. It was found that the longer piles increased the FoS value. However, once the critical length was exceeded, the FoS value tended to remain constant.

In addition, slope reinforcement using a double-row pile configuration has been analysed by several researchers, such as Munawir et al. [21] studied slopes reinforced with double-row piles using finite element analysis. The results showed that the double-row pile configuration enhanced the slope's resistance to failure, as evidenced by a 29.05% increase in the safety factor (FoS) compared to an unreinforced slope. Meanwhile, compared to a single-row installation pattern, it increased the FoS value by 4.38%. According to Lei et al. [22] slopes reinforced with double-row piles are less likely to experience severe damage, are easier to repair, and exhibit improved anti-slip mechanical characteristics.

Based on the above discussion, it is clear that single-row and double-row installation patterns contribute to maintaining slope stability, as indicated by an increase in the SoF value. However, there are no slope reinforcements using other installation patterns, such as the U-shape. Therefore, the aim of this study is to analyze the stability of slopes reinforced with piles in a U-shape configuration numerically and compare the results with the existing conditions of the unreinforced slope. The method used is finite element analysis with the strength reduction method (SRM).

II. Research Method

A. Site Investigation and Assessment

Field investigations were conducted to determine the site conditions, geology, and geotechnical characteristics in the vicinity of the project location. These activities also played a crucial role in characterizing soil profiles for geotechnical planning [23]. The field investigations that were conducted included visual observations, geophysical surveys, GPR, and geotechnical investigations.

1) Visual Assessment

Visual observations were used to identify geological conditions in the form of cracks, including crack width, length, and depth. These observations played a significant role as a decision-making method, for risk control, and as a preventive measure in slope engineering. Additionally, they were served as supplementary data for identifying critical areas on the slope. The visual method used was traditional 2D data and geographic information obtained using unmanned aerial vehicles (UAVs) or photogrammetry [24].

2) Geoelectrical Test

Field investigations using geophysical methods were also performed to support data collection or to assess geological conditions around the observation site, such as geoelectric surveys. The purpose of geoelectric surveys was to examine weak zones beneath the ground surface on slopes. Surface geoelectric resistivity surveys were calibrated with resistivity measurements to improve the interpretation of electrical resistivity [25]. This study detected the effects of induced electric currents transmitted by the soil. The mechanism of this research was based on measurements of electrical potential at the surface, which depended on the distribution of electrical resistivity [26]–[27].

3) Georadar

Furthermore, another geophysical survey method that played a significant role was ground-penetrating radar (GPR). For many years, this method has been one of the best techniques for non-destructive investigation. The purpose of GPR surveys was to evaluate ground surface conditions and the existing state of materials through GPR numerical simulations based on wave velocity reduction. GPR consisted of transmitters, receivers, and control units to trigger, control, and record EM wave pulses, as shown in Fig. 1 dan Fig. 2. In the implementation, this survey used two types of wave frequencies for GPR profiling. First, high-frequency waves (700 MHz) produced high-resolution images but they were limited to shallow penetration depths. Second, low-frequency waves reached deep penetration but produced low-resolution images [28].



Fig. 1. Georadar antenna GSSI 350 MHz

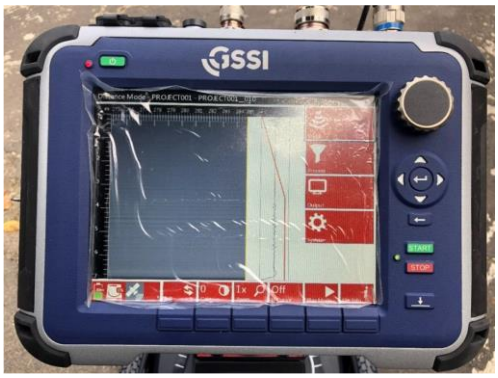


Fig. 2. Georadar main unit SIR4000

4) Geotechnical Investigation

Besides geophysical investigations, geotechnical investigations were also required to evaluate the physical and mechanical parameters of the soil. These investigations included Cone Penetration Test (CPT), Standard Penetration Test (SPT), and laboratory testing [29]. The standard used for CPT testing was ASTM D5778, while SPT testing was based on ASTM D1586. Meanwhile, laboratory testing was performed to determine the physical and mechanical parameters of the soil. The tests conducted are shown in TABLE I and TABLE II.

TABLE I. PHYSICAL PROPERTIES TEST OF SOIL

Laboratory test	Reference
Water content	ASTM D265
Specific gravity	ASTM D854
Density	ASTM D2937
Atterberg limit	ASTM D424
Grain size analysis	ASTM D4318

TABLE II. MECHANICAL PROPERTIES TEST OF SOIL

Laboratory test	Reference
Direct shear	ASTM D3080
Consolidation	ASTM D2435

B. Finite element analysis

Finite element analysis (FEA) using the strength reduction method (SRM) is a method used in slope stability analysis that determines the stability condition of soil or rock masses by progressively reducing the material strength parameters (cohesion and friction angle) until failure occurs. Moreover, the finite element method approach offered advantages in slope stability analysis, as it required no assumptions in calculations regarding slip planes, failure modes, or the division of soil layers. Furthermore, this method enabled analysis of slopes with complex stratigraphic and geomorphological conditions. This approach was also capable of analysing nonlinear soil deformation. Consequently, it provided a detailed, comprehensive simulation of damage resulting from the formation of surface cracks due to displacement [14], [30].

In this study, two stages of analysis were conducted. The first stage involved numerical analysis of the existing conditions to determine slope stability prior to reinforcement. The second stage included numerical analysis of the slope after reinforcement with piles. The purpose was to reveal the influence of piles with a U-shape installation configuration. The analysed results consisted of safety factor values compared to applicable standard requirements.

III. RESULT AND DISCUSSION

A. Site Condition

1) Topographic Conditions

The research object was a slope where an Extra High Voltage (EHV) power line network with tower code T.388 was constructed. The research location was in Ungaran City, Central Java Province, Indonesia. The topographic conditions of the area consisted of a steep slope adjacent to mining sites on the right and left, as shown in the site maps in Fig. 3 dan Fig. 4.



Fig. 3. Slope condition near T.388 Tower

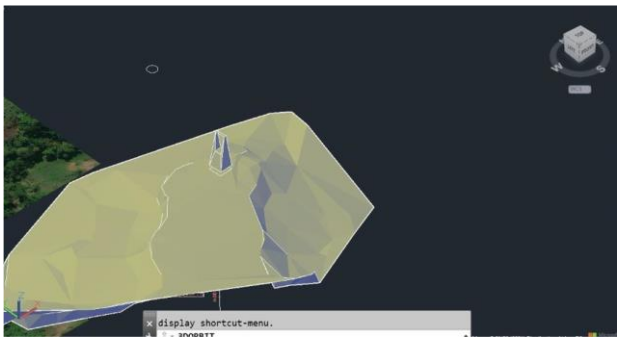


Fig. 4. Place of T.388 Tower

A visual observation based on aerial photographs taken using a drone revealed a 30-centimeter-wide crack extending 6 meters from the tower. The crack was caused by mining excavation activities around the tower, which was exposed to the environment without any protection for the slope surface. The tower structure was also weakened by ground movement. This condition is confirmed by the aerial photograph shown in Fig. 5. The thin red line indicates the length of the crack around the tower.



Fig. 5. Crack along the tower

2) Geotechnical Properties

Several types of geotechnical investigations were also conducted to provide the data required for slope stability analysis, including SPT, CPT, and laboratory tests. SPT testing was performed at one location to a depth of 30 m with a penetration interval of 2 m, while CPT testing was conducted at four locations with an average depth of hard soil at 2.8 m. Based on laboratory testing, it was confirmed that the soil conditions around the project site are dominated by silt mixed with clay and sand. The results of the laboratory testing are shown in

TABLE *III*.

TABLE III. SOIL STRENGTH PARAMETER

Depth (m)		Layer	NSPT	γ	Shear strength		Drained strength		
				(kN/m^3)	Cu (kPa)	Ø (°)	C´(kPa)	Ø´ (°)	E (kPa)
0	7	Clayey silt	21	18	80	0	2	23	10000
7	18	Sandy silt	56	19	300	0	3	26	20000
18	25	Silty sand	60	19	3	35	3	35	70000
25	30	Silt	60	19	360	0	35	27	100000

3) Subsurface Classification

Electrical resistivity testing was used to evaluate the condition of subsurface layers—specifically, the types of materials beneath the surface around the observation site—by utilizing high-voltage DC current. Two tracks were analysed, each with a maximum span of 215 m. The results of the geophysical survey interpretation for traverse one are shown in Fig. 7. Meanwhile, the interpretation of the geophysical survey for traverse two is shown in Fig. 8. In the 3D view, geophysical survey traces 1 and 2 are shown in Fig. 6.

The output generated from the geophysical survey consisted of elongated cross-sections of the soil containing images with specific colour codes. The colour selection was grouped based on resistivity values and soil type classifications. Green indicated sandy clay soil with resistivity <25 ohm.m, while yellow represented tuffaceous clay-gravel soil with resistivity 25–50 ohm.m. m, dark grey indicated sandy and gravelly clay with resistivity of 50–300 ohm·m, and red denoted gravel, breccia fractures, and sandstone with resistivity >300 ohm.m [31]. The standard resistivity values for soil and rock materials used to determine the type of soil beneath an EHV power line are shown in TABLE II.

TABLE IV. MECHANICAL PROPERTIES TEST OF SOIL [32]

Material	Resistivity (ohm.m)
Alluvium	10 – 80
Sand	60 – 100
Clay	1 – 100
Groundwater (fresh)	10 – 100
Sandstone	8 – 4 x 10^3
Shale	20 – 2 x 10^3
Limestone	50 – 4 x 10^3
Granite	5000 - 10^6

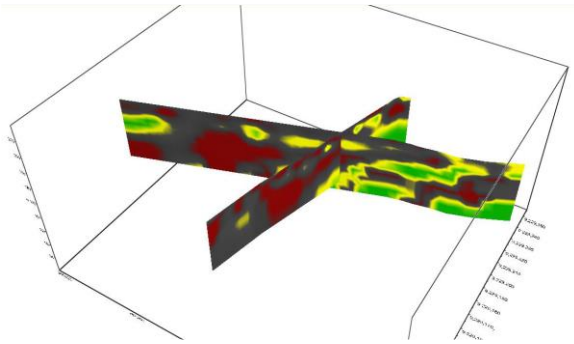


Fig. 6. 3D Model on Geoelectrical Test

Based on the analysis of the soil layers on Runway 1 shown in Fig. 9, it was found that in general, these soil layers fell into the categories of sandy soil, clay, and gravel.

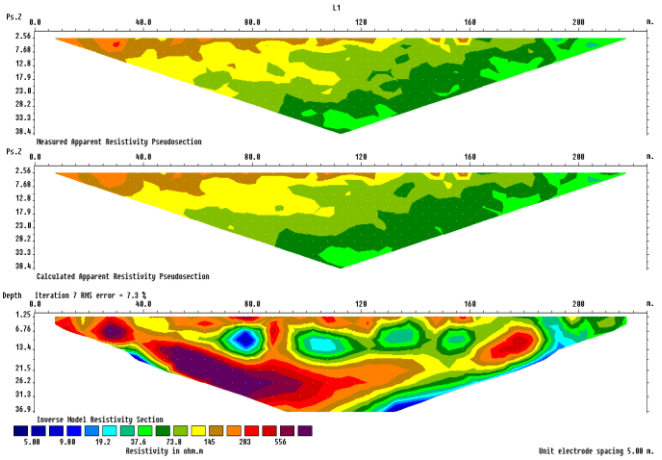


Fig. 7. Geoelectrical interpretation along line 1

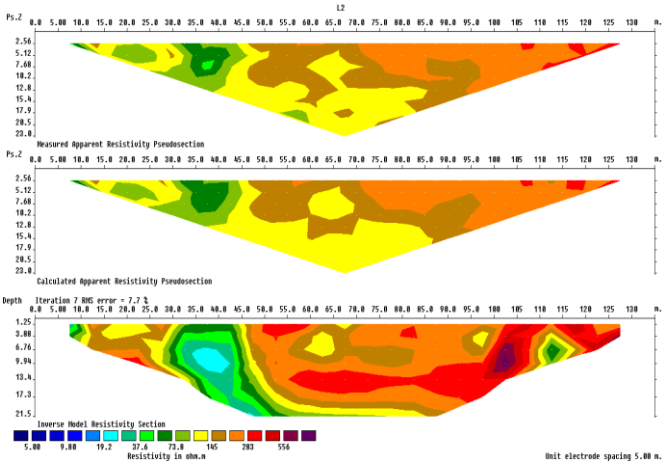


Fig. 8. Geoelectrical interpretation along line 2

This pattern was indicated by the presence of green and yellow colour patterns, as well as a few red patterns. Besides that, the soil characteristics of Section 1, marked by green colour patterns in the southwest-to-northeast direction or at the end of the section, indicated that the soil layers were prone to shifting when subjected to significant pressure, even though there were hard layers present. Layers with yellow colour patterns were identified at the 180-meter mark, which sloped down toward the mining route from the area of Tower T.388 [31].

Meanwhile, on Section 2 shown in Fig. 10, it was found that in general, the soil layers were categorized as sand, clay, and gravel. The layers were marked by the presence of green and yellow colour patterns, as well as a few red patterns. The characteristics of the soil in section 2, marked by yellow and green patterns in the western or initial part of the section, indicated that the soil layer was prone to shifting under significant pressure, even though a hard layer was present. The layer with yellow pattern was identified at the 40-meter mark near the T.388 tower area [31].

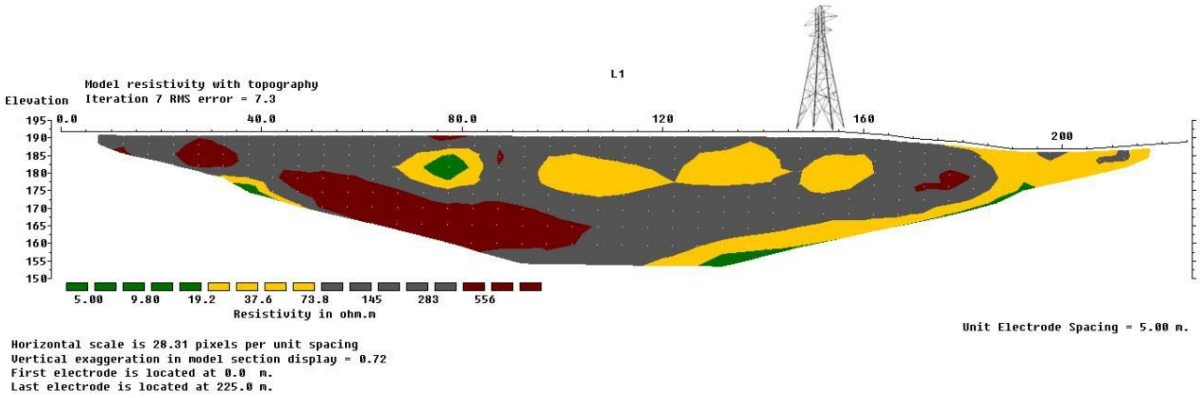


Fig. 9. Layer analysis in line 1

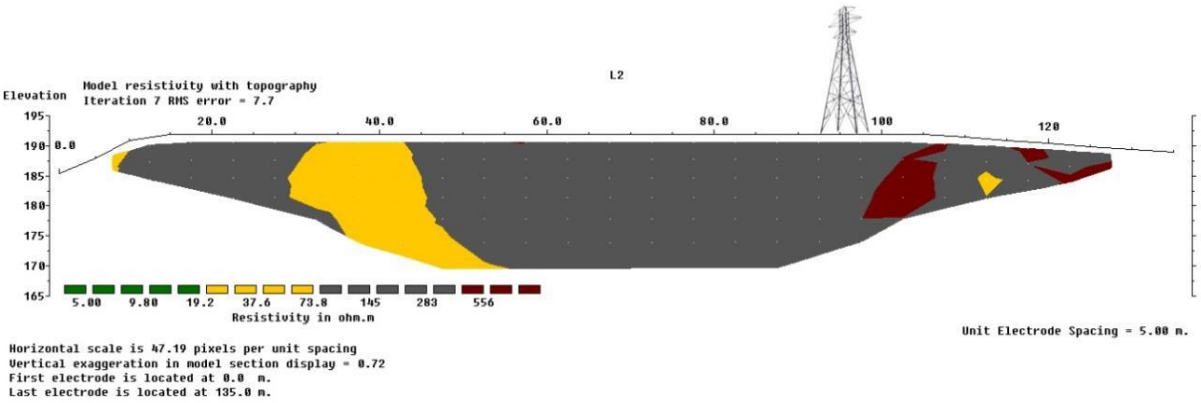


Fig. 10. Layer analysis in line 2

4) Condition of Existing Structure

Georadar survey was performed to identify the condition of the subsurface structure (foundation) and cracks along the survey area of the EHV power line adjacent to a steep slope. The survey was conducted around the base of the tower shown in Fig. 11.

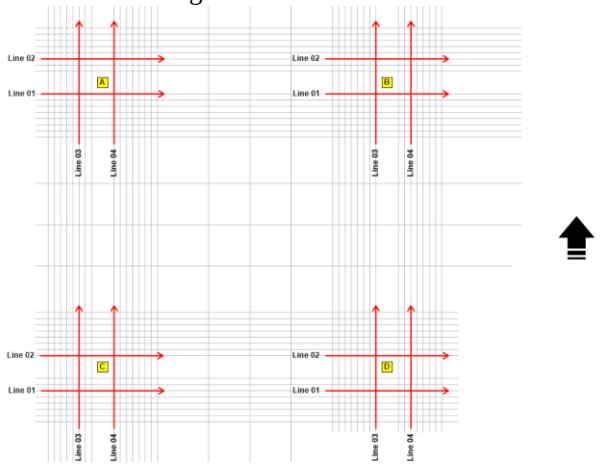


Fig. 11. Interpretation result of georadar investigation

Based on the results of the field study using ground-penetrating radar, it was revealed that four foundation points were detected at depths of 0.4 – 7.7 m. The dimensions of the detected foundations were 3.7 x 3.7 m. From the frequencies captured by the ground-penetrating radar, no significant cracks or fractures were found in the tower foundations. This condition was indicated by wave diffraction patterns shown in Fig. 12-Fig. 15. Consequently, no reinforcement or retrofitting was required for the Extra High Voltage (EHV) Power Line structure.

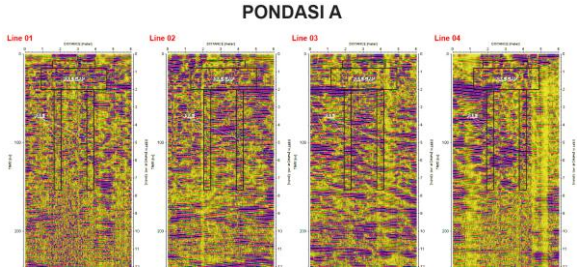


Fig. 12. Foundation Interpretation on point A

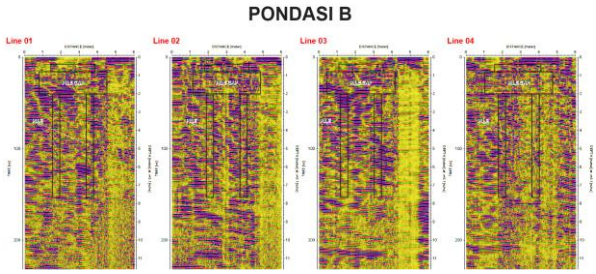


Fig. 13. Foundation Interpretation on point B

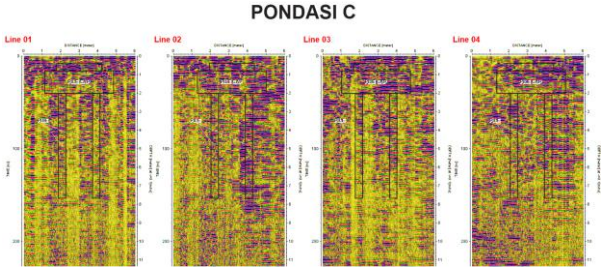


Fig. 14. Foundation Interpretation on point C

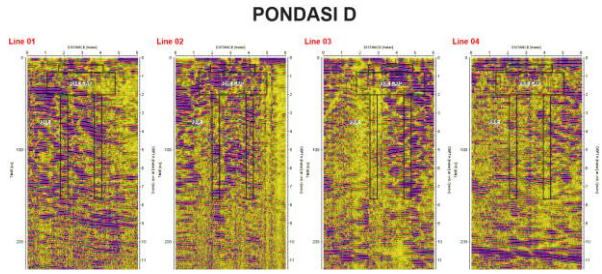


Fig. 15. Foundation Interpretation on point D

B. Numerical Analysis

1) Existing Slope

The numerical analysis was assisted by Plaxis 2D software, in which the slope was modeled based on a previously conducted field survey. The slope model was designed to be similar to the actual conditions in the field to obtain representative results. Fig. 16-Fig. 18 show the topographic conditions around the observation site, which experienced severe deformation, as well as the modeling of the Extra High Voltage (EHV) Power Line foundation to analyze soil behavior due to the distribution of stress occurring under existing conditions.

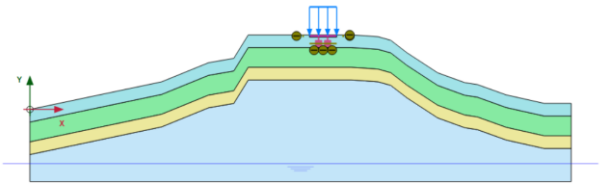


Fig. 16. Section A-A' on Plaxis model

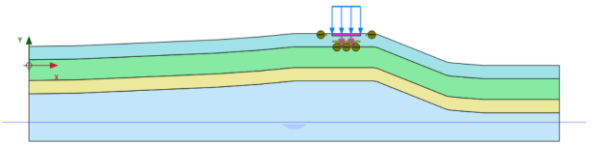


Fig. 17. Section B-B' on Plaxis model

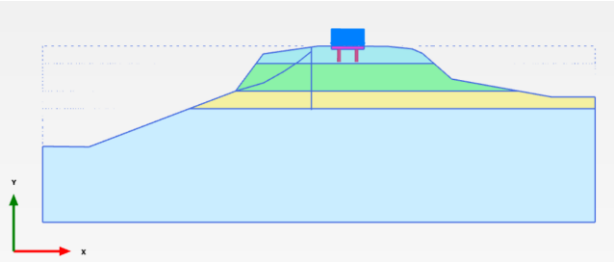


Fig. 18. Section C-C' on Plaxis model

The results of the finite element analysis in TABLE V show that the safety factor values for the existing slope ranged from 1.22 to 1.48. The lowest safety factor (FoS) value was observed in the C-C' slope section. Meanwhile, the largest FoS value was shown in the B-B' slope section. This occurred due to open-cut excavation activities in the mining operation, which caused displacement and deformation toward the excavation pit. This displacement resulted from soil pressure caused by the soil mass due to dead load or excess load [33].

Therefore, based on SNI 8640:2017 established by the Indonesian government, the slope is at risk of failure because it has a safety factor of less than 1.5 for permanent earth slopes. Furthermore, according to FHWA-NHI–06-088 established by the U.S. Department of Transportation, the Federal Highway Administration states that the slope's condition falls into the critical category. This is because the safety factor of the existing slope is lower than the specified requirement of 1.5, making it prone to severe damage [34].

TABLE V.
SAFETY FACTOR VALUES AT INITIAL CONDITION

Section	Condition	FoS	Note
A-A'	Existing	1.43	Unstable
B-B'	Existing	1.48	Unstable
C-C'	Existing	1.22	Unstable

2) Reinforced Slope

Slope reinforcement is intended to improve stability, as indicated by the safety factor. Under existing conditions, the entire slope section had a value below the required standard. Therefore, reinforcement work was necessary. One of the reinforcement methods used involved the installation of piles. In this study, the piles used were concrete bored piles with a diameter of 400 mm, and the spacing between pile centers was 400 mm. The pile installation system used was a double contiguous pile system with a U-shaped configuration, where the piles were installed adjacent to one another. The arrangement of the bored piles is shown in Fig. 19.

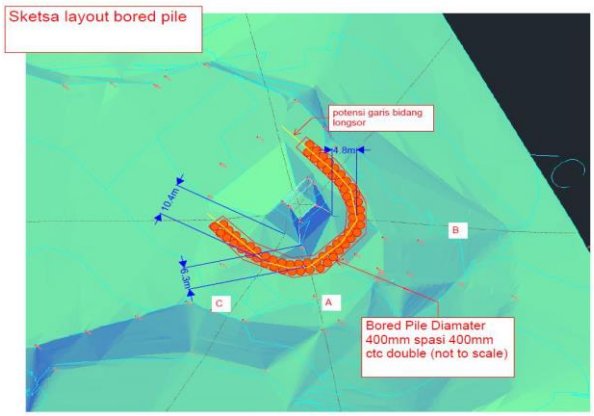


Fig. 19. Section A-A' on Plaxis model

TABLE VI shows the safety factor values for slopes reinforced with piles. The results revealed that the U-shaped installation pattern affected slope stability. This showed up in the increase in FoS values across all slope sections—A-A', B-B', and C-C'. In section A-A', there was a 9% increase. Meanwhile, in section B-B', the FoS value showed an improvement of 3.5%. Additionally, section C-C' demonstrated a significant increase in the FoS value, rising from 1.22 to 2.04 with 57% increase. This aligned with research conducted by Munawir (2024), which revealed that reinforcement with piles improved the stability of steep sandy slopes, as indicated by an increase in the FoS value [35]. The comparison of FoS values before and after reinforcement using piles is shown in Fig. 20.

The effects of slope reinforcement using piles included increased compression and reduced shear. The presence of piles also inhibited deformation and reduced slope inclination localization. In this case, the load on the unstable soil was transferred to the rigid boundaries of the piles. Consequently, this event resulted in an increase in the FoS value [36]. In addition, the spacing between posts also played a role: the closer the spacing between posts, the

greater the slope stability, as this promoted the arching effect of the soil [37]. Furthermore, the critical slip surface also shifted toward the slope due to the reduced spacing between posts [38].

TABLE VI. SAFETY FACTOR VALUES AFTER REINFORCEMENT

Section	Condition	FoS	Note
A-A'	Existing	1.56	Stable
B-B'	Existing	1.53	Stable
C-C'	Existing	2.04	Stable

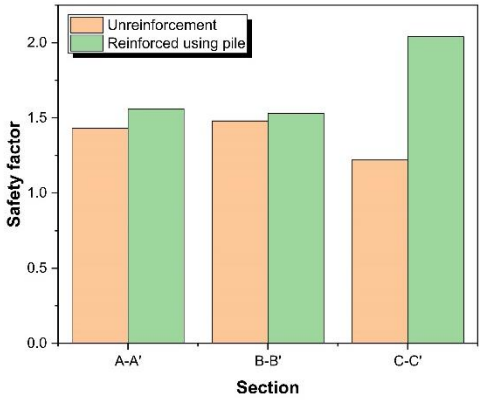


Fig. 20. Comparison of FoS Value

V. CONCLUSION

The results of a series of tests, such as electrical resistivity surveys, georadar, and borehole logs, indicated that the slope consists of a mixture of sandy clay and a small amount of gravel. Mining activities contributed to slope displacement and the potential for continuous deformation. Therefore, Slope reinforcement using piles arranged in a U-shaped pattern had a positive effect on slope stability, as indicated by an increase in the safety factor (FoS) values up to 57% across the entire slope section. This increase in FoS values occurred because the presence of the piles was able to inhibit the deformation occurring on the slope by transferring the load from the loose soil to the rigid boundaries of the pile. As a result, slopes that are reinforced with U-shaped piles comply with the slope stability standards set out in SNI 8640:2017.

REFERENCES

[1] S. Regmi and R. K. Dahal, "Consequences of slope instability and existing practices of mitigation in hydropower projects of Nepal," *Geoenviron. Disasters*, vol. 11, no. 1, e26, Sep. 2024, doi: 10.1186/s40677-024-00289-2.

[2] Y. A. Nanehkaran *et al.*, "Comparative analysis for slope stability by using machine learning methods," *Appl. Sci.*, vol. 13, no. 3, e1555, Jan. 2023, doi: 10.3390/app13031555.

[3] M. Kassa and M. Meten, "Slope stability analysis using kinematic, limit equilibrium, and finite element models at Dessie town, northern Ethiopia," *Arab J. Geosci.*, vol. 16, no. 12, e675, Dec. 2023, doi: 10.1007/s12517-023-11783-6.

[4] W. F. Chen and N. Snitbhan, "On slip surface and slope stability analysis," *Soils and Foundations*, vol. 15, no. 3, pp. 41–49, Sep. 1975, doi: 10.3208/sandf1972.15.3_41.

[5] G. Song, X. Song, S. He, D. Kong, and S. Zhang, "Soil reinforcement with geocells and vegetation for ecological mitigation of shallow slope failure," *Sustain.*, vol. 14, no. 19, e11911, Sep. 2022, doi: 10.3390/su141911911.

[6] X. Cai *et al.*, "Dynamic characteristics of reinforced soil retaining wall with composite gabion based on time domain identification method," *Sustain.*, vol. 14, no. 23, e16321, Dec. 2022, doi: 10.3390/su142316321.

[7] B. Evirgen, H. O. Kara, M. S. Ucun, A. A. Gültekin, M. Tos, and V. Öztürk, "The effect of the geometrical properties of geocell reinforcements between a two-layered road structure under overload conditions," *Case Stud. in Construction Materials*, vol. 20, e02793, Jul. 2024, doi: 10.1016/j.cscm.2023.e02793.

[8] E. Ngii and A. Minmahddun, "Safety enhancement of eroded gabion wall using optimized mini-piles," *Geomate*, vol. 29, no. 133, Sep. 2025, doi: 10.21660/2025.133.5047.

[9] Z. Chen *et al.*, "Recent advances in high slope reinforcement in China: Case studies," *J. Rock Mechanic Geotech. Eng.*, vol. 8, no. 6, pp. 775–788, Dec. 2016, doi: 10.1016/j.jrmge.2016.11.001.

[10] Z. Du, Y. Zhang, H. Huo, S. Shi, R. Li, and B. Han, "Green anchors enhance slope stability: mechanisms and efficacy in reinforcement," *Earthq. Res. Adv.*, vol. 5, no. 3, e100372, Jul. 2025, doi: 10.1016/j.eqrea.2025.100372.

[11] H. Marwane *et al.*, "Soil nailing for slope stabilization: An overview," *Interactions*, vol. 246, no. 1, e14, Dec. 2024, doi: 10.1007/s10751-024-02234-z.

[12] B. R. Pandey, H. Knoblauch, and G. Zenz, "Slope stability evaluation due to reservoir draw-down using LEM and stress-based FEM along with Mohr–Coulomb criteria," *Water*, vol. 15, no. 22, e4022, Nov. 2023, doi: 10.3390/w15224022.

[13] D. A. Bouzid, "Finite element analysis of slope stability by expanding the mobilized principal stress Mohr's circles – Development, encoding and validation," *J. Rock Mechanics Geotech. Eng.*, vol. 14, no. 4, pp. 1165–1179, Aug. 2022, doi: 10.1016/j.jrmge.2022.01.016.

[14] S. Harabinova, K. Kotrasova, and E. Panulinova, "Comparison of limit equilibrium and finite element method for slope stability analysis," *Buildings*, vol. 16, no. 3, e577, Jan. 2026, doi: 10.3390/buildings16030577.

[15] M. C. Irnawan, Y. Zaika, and A. Munawir, "Interaction of composite material-based geopolymer with soil in road pavement using finite element method," *Rekayasa Sipil*, vol. 19, no. 3, pp. 275–282, Sep. 2025, doi: 10.21776/ub.rekayasasipil.2025.019.03.2.

[16] S. Y. Liu, L. T. Shao, and H. J. Li, "Slope stability analysis using the limit equilibrium method and two finite element methods," *Comput. Geotech.*, vol. 63, pp. 291–298, Jan. 2015, doi: 10.1016/j.compgeo.2014.10.008.

[17] T. Garo, M. Tesfaye, and S. Karuppannan, "Slope stability modeling using limit equilibrium and finite element methods: A case study of the Adama City, Northern main Ethiopian rift," *Quaternary Sci. Adv.*, vol. 15, e100228, Sep. 2024, doi: 10.1016/j.qsa.2024.100228.

[18] M. Guo, J. Li, and X. Dong, "Determining the critical slip surface of slope by vector sum method based on strength reduction definition," *Front. Earth Sci.*, vol. 10, e865017, Apr. 2022, doi: 10.3389/feart.2022.865017.

[19] W. B. Wei and Y. M. Cheng, "Strength reduction analysis for slope reinforced with one row of piles," *Comput. Geotech.*, vol. 36, no. 7, pp. 1176–1185, Sep. 2009, doi: 10.1016/j.compgeo.2009.05.004.

[20] I. Shooshpasha and H. A. Amirdehi, "Evaluating the stability of slope reinforced with one row of free head piles," *Arab J. Geosci.*, vol. 8, no. 4, pp. 2131–2141, Apr. 2015, doi: 10.1007/s12517-014-1272-7.

[21] A. Munawir, "Double-row pile reinforcing on a critical slope at national road in Tabanan, Bali," *Geomate*, vol. 26, no. 115, Mar. 2024, doi: 10.21660/2024.115.4276.

[22] H. Lei, X. Liu, Y. Song, and Y. Xu, "Stability analysis of slope reinforced by double-row stabilizing piles with different locations," *Nat. Hazards*, vol. 106, no. 1, pp. 19–42, Mar. 2021, doi: 10.1007/s11069-020-04446-2.

[23] R. Yang, J. Huang, D. V. Griffiths, J. Meng, and G. A. Fenton, "Optimal geotechnical site investigations for slope design," *Computers and Geotechnics*, vol. 114, e103111, Oct. 2019, doi: 10.1016/j.compgeo.2019.103111.

[24] X. Jian, "Slope visualisation and stability study using geographic information science," *Geotech. Res.*, vol. 11, no. 3, pp. 112–122, Sep. 2024, doi: 10.1680/jgere.23.00030.

[25] N. Islami, "Detection of the soft soil at the slope area using geoelectrical resistivity method," *J. Phys.: Conf. Ser.*, vol. 1351, no. 1, e012044, Nov. 2019, doi: 10.1088/1742-6596/1351/1/012044.

[26] L. Marescot, R. Monnet, and D. Chapellier, "Resistivity and induced polarization surveys for slope instability studies in the Swiss Alps," *Eng. Geology*, vol. 98, no. 1–2, pp. 18–28, Apr. 2008, doi: 10.1016/j.enggeo.2008.01.010.

[27] M. A. Antareza, A. Wafi, Y. Lasmana, and M. Mariyanto, "Geoelectrical survey and cone penetration test data for groundwater potential determination around Gatot Subroto Street, Banjarmasin," *J. Phys.: Conf. Ser.*, vol. 1825, no. 1, e012015, Feb. 2021, doi: 10.1088/1742-6596/1825/1/012015.

[28] M. Elkarmoty, H. E. Allam, K. Helal, F. Ahmed, S. Bonduà, and S. A. Mourad, "Georadar survey and simulation for subsurface investigation at historical Mosque of Sorghatmesh, Cairo, Egypt," *Buildings*, vol. 14, no. 11, e3653, Nov. 2024, doi: 10.3390/buildings14113653.
[29] T. C. Irunkwor *et al.*, "Geoelectric and geochemical assessment of sub-soil corrosivity and competence for civil infrastructures at Utue-Ogume, Delta State, Nigeria," *Discov Geosci*, vol. 3, no. 1, e149, Oct. 2025, doi: 10.1007/s44288-025-00256-w.
[30] Y. Gu, Y. Yuan, K. Xue, Y. Yin, S. Lu, and X. Jiang, "A novel strength reduction method for a slope stability assessment based on a finite element method," *Processes*, vol. 12, no. 10, e2273, Oct. 2024, doi: 10.3390/pr12102273.
[31] P. Petrov, G. Velev, and K. Ivanov, "Approach for preliminary determination of the type and number of vertical rods in grounding installations," *E3S Web Conf.*, vol. 168, e00013, 2020, doi: 10.1051/e3sconf/202016800013.
[32] S. N. M. Akip Tan, M. F. Md Dan, M. E. Tonnizam, R. Saad, A. Madun, and Z. A. M. Hazreek, "Interpretation of 2D resistivity with engineering characterisation of subsurface exploration in Nusajaya Johor, Malaysia," *J. Phys.: Conf. Ser.*, vol. 995, e012078, Apr. 2018, doi: 10.1088/1742-6596/995/1/012078.
[33] B. Lan, Y. Wang, and W. Wang, "Review of the double-row pile supporting structure and its force and deformation characteristics," *Applied Sciences*, vol. 13, no. 13, e7715, Jun. 2023, doi: 10.3390/app13137715.
[34] C. Arriola *et al.*, "Physical slope stability: Factors of safety under static and pseudo-static conditions," *Infrastructures*, vol. 10, no. 3, e53, Mar. 2025, doi: 10.3390/infrastructures10030053.
[35] A. Munawir, "The slope stability of sand slope with two rows pile reinforcing," *Geomate*, vol. 24, no. 103, Mar. 2023, doi: 10.21660/2023.103.3572.
[36] S. Liu, F. Luo, and G. Zhang, "Pile reinforcement behavior and mechanism in a soil slope under drawdown conditions," *Bull Eng. Geol. Environ.*, vol. 80, no. 5, pp. 4097–4109, May 2021, doi: 10.1007/s10064-021-02191-9.
[37] P. Gupta and S. Mehndiratta, "Exploring the efficacy of slope stabilization using piles: A comprehensive review," *Indian Geotech. J.*, vol. 55, no. 5, pp. 3442–3459, Oct. 2025, doi: 10.1007/s40098-024-01119-w.
[38] G. Zhang and L. Wang, "Simplified evaluation on the stability level of pile-reinforced slopes," *Soils and Foundations*, vol. 57, no. 4, pp. 575–586, Aug. 2017, doi: 10.1016/j.sandf.2017.03.009.



Muhammad Chofi Irnawan, M. T. is a lecturer in the Study Program of Civil Engineering, Universitas Widya Kartika. He is a lecturer in the Geotechnical Engineering expertise group. His research focuses on Geotechnical Engineering, Soil Mechanics, soil improvement, soil Stability, and Slope Stability. (email: chofiirnawan@gmail.com).



Muhammad Shofwan Donny Cahyono, M. T. is a lecturer and head of the study program in the Study Program of Civil Engineering, Universitas Widya Kartika. He is a lecturer in the Transportation Engineering expertise group. His research focuses on Transportation, Pavement Engineering, Geotechnics, and Slope Stability. (email: shofwandonny@widyakartika.ac.id).